Supporting Information for:

A Highly Selective Red-emitting FRET Fluorescent Molecular Probe Derived From BODIPY for the Detection of Cysteine and Homocysteine: An Experimental and Theoretical Study

Jingyin Shao,[†] Haiyang Sun,[†] Huimin Guo[†], Shaomin Ji, [†] Jianzhang Zhao,[†*] Wenting Wu,[†] Xiaolin Yuan,[¶] Chunlei Zhang, [¶] Tony D. James [§*]

[†]State Key Laboratory of Fine Chemicals, School of Chemical Engineering, Dalian University of Technology, E-208 West Campus, 2 Ling-Gong Road, Dalian 116024, P. R. China; [¶] Center Laboratory, Affiliated Zhongshan Hospital of Dalian University, Dalian 116001, P. R. China and [§] Department of Chemistry, University of Bath, Bath BA2 7AY, United Kingdom.

E-mail: zhaojzh@dlut.edu.cn (J.Z.) and t.d.james@bath.ac.uk (T.J.)

Group homepage (J. Zhao): http://finechem.dlut.edu.cn/photochem

Index

Experimental Section

General

NMR spectra were taken on a 400 MHz Varian Unity Inova spectrophotometer. Mass spectra were recorded with a Q-TOF Micro MS spectrometer. UV-Vis spectra were taken on a HP8453 UV-visible spectrophotometer. Fluorescence spectra were recorded on a JASCO FP-6500 or a RF5301 PC (Shimadzu) spectrofluorometer. Luminescence quantum yields were measured with quinine bisulfate in 0.05 M H_2SO_4 (F = 54.6%). Luminescence lifetimes were measured on a Horiba Jobin Yvon Fluoro Max-4 (TCSPC) instrument. The cells luminescence images were obtained using a Nikon ECLIPSE-Ti confocal laser scanning microscopy.

The structures of complexes were optimized using density functional theory (DFT) with B3LYP functional and 6-31G(d) basis set. The excited state related calculations were carried out with the time dependent DFT (TD-DFT) with the ground state geometry. The 6-31G(d) basis set was employed for C, H, N, O, S. There are no imaginary frequencies for all optimized structures. All the DFT/TDDFT calculations were performed using Gaussian 09W. [1]

Reference:

1. Gaussian 09W, Revision A.1, M. J. Frisch, G. W. Trucks, H. B. Schlegel, G. E. Scuseria, M. A. Robb, J. R. Cheeseman, G. Scalmani, V. Barone, B. Mennucci, G. A. Petersson, H. Nakatsuji, M. Caricato, X. Li, H. P. Hratchian, A. F. Izmaylov, J. Bloino, G. Zheng, J. L. Sonnenberg, M. Hada, M. Ehara, K. Toyota, R. Fukuda, J. Hasegawa, M. Ishida, T. Nakajima, Y. Honda, O. Kitao, H. Nakai, T. Vreven, J. A. Montgomery, Jr., J. E. Peralta, F. Ogliaro, M. Bearpark, J. J. Heyd, E. Brothers, K. N. Kudin, V. N. Staroverov, R. Kobayashi, J. Normand, K. Raghavachari, A. Rendell, J. C. Burant, S. S. Iyengar, J. Tomasi, M. Cossi, N. Rega, J. M. Millam, M. Klene, J. E. Knox, J. B. Cross, V. Bakken, C. Adamo, J. Jaramillo, R. Gomperts, R. E. Stratmann, O. Yazyev, A. J. Austin, R. Cammi, C. Pomelli, J. W. Ochterski, R. L. Martin, K. Morokuma, V. G. Zakrzewski, G. A. Voth, P. Salvador, J. J. Dannenberg, S. Dapprich, A. D. Daniels, Ö. Farkas, J. B. Foresman, J. V. Ortiz, J. Cioslowski, and D. J. Fox, Gaussian, Inc., Wallingford CT, **2009**.

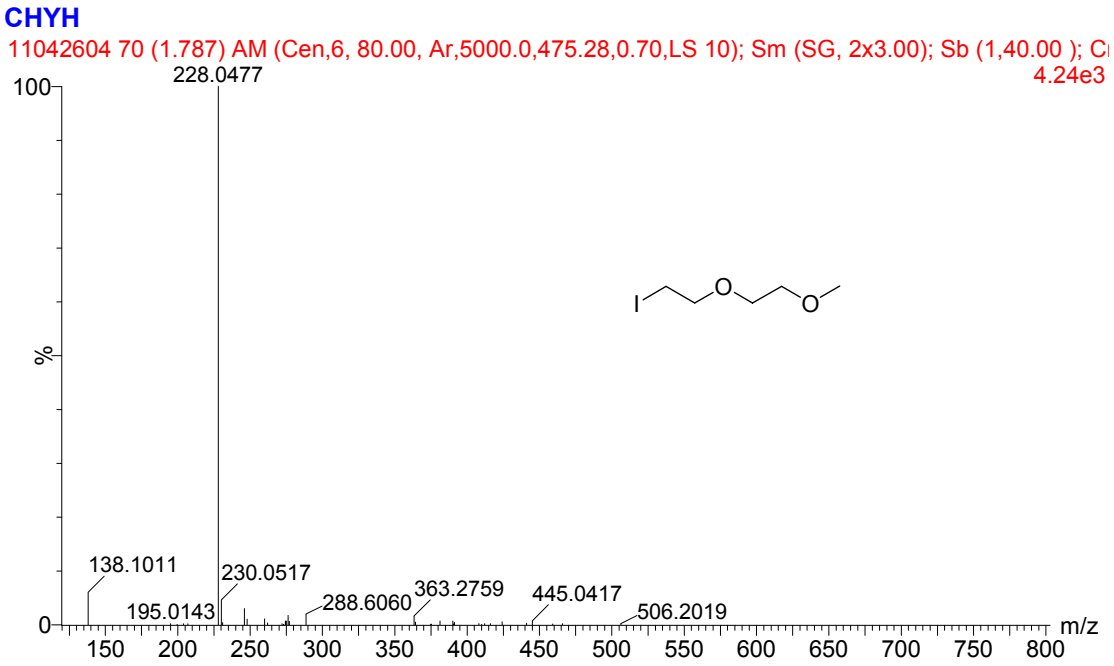

Figure S1. TOF MS EI of **1**.

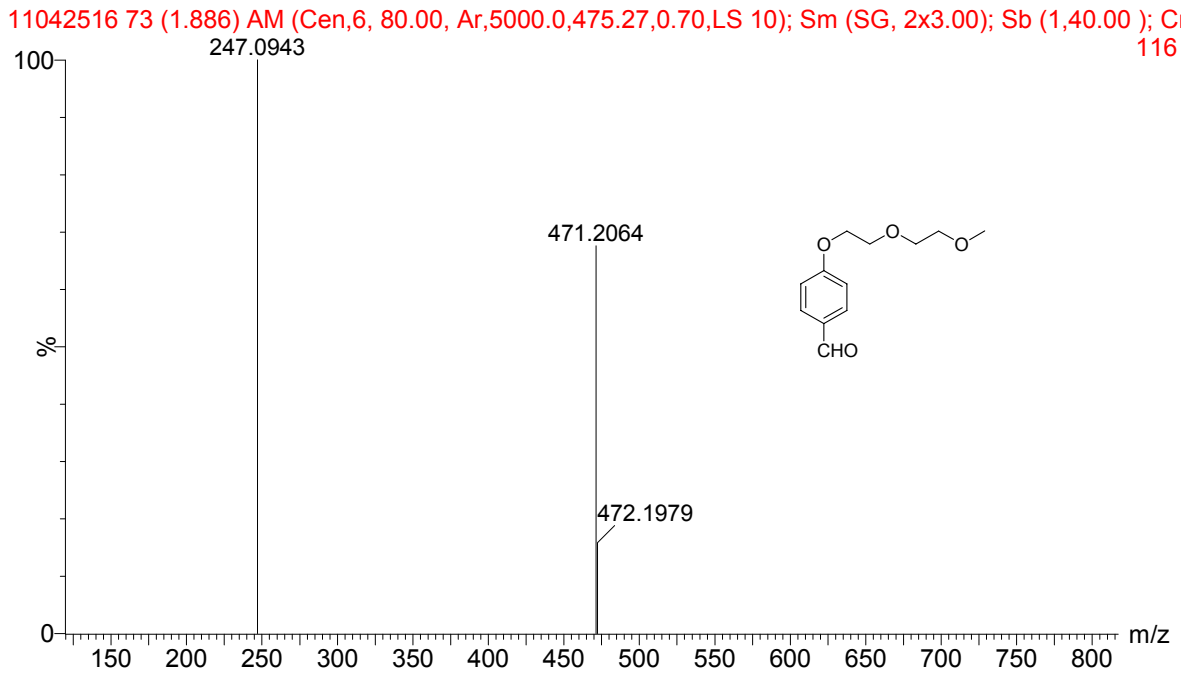

Figure S2. TOF MS EI of **2**.

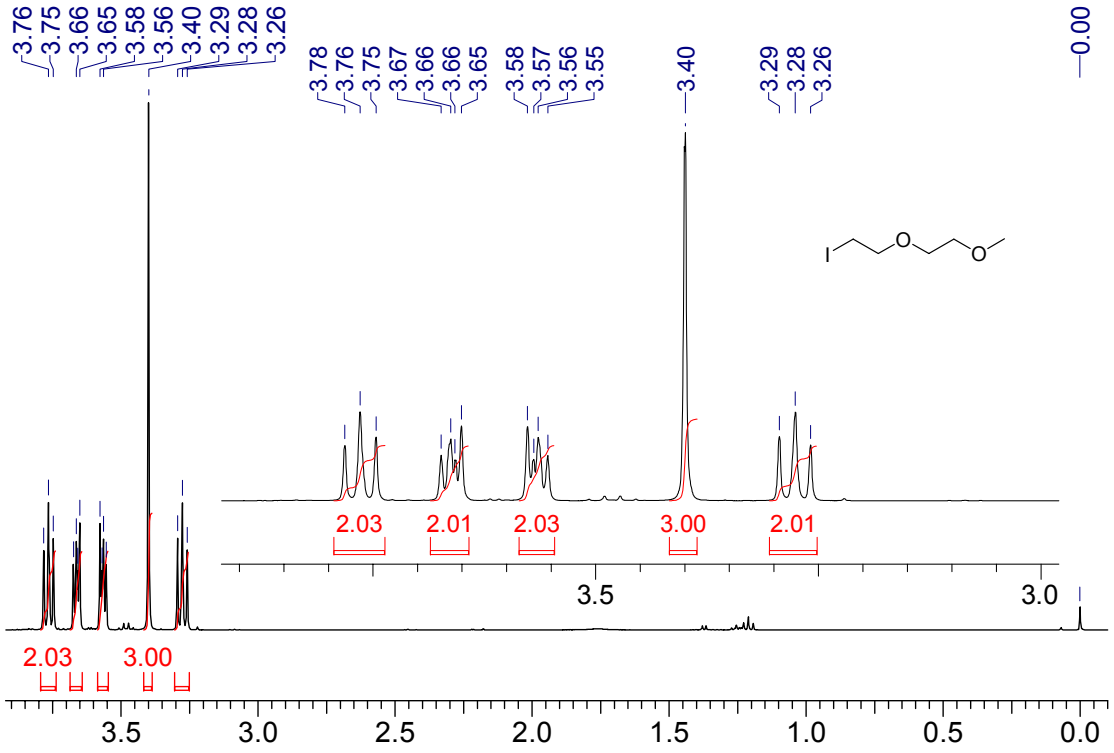

Figure S3. ^{1}H NMR of **1** ($CDCl_3$, 400 MHz).

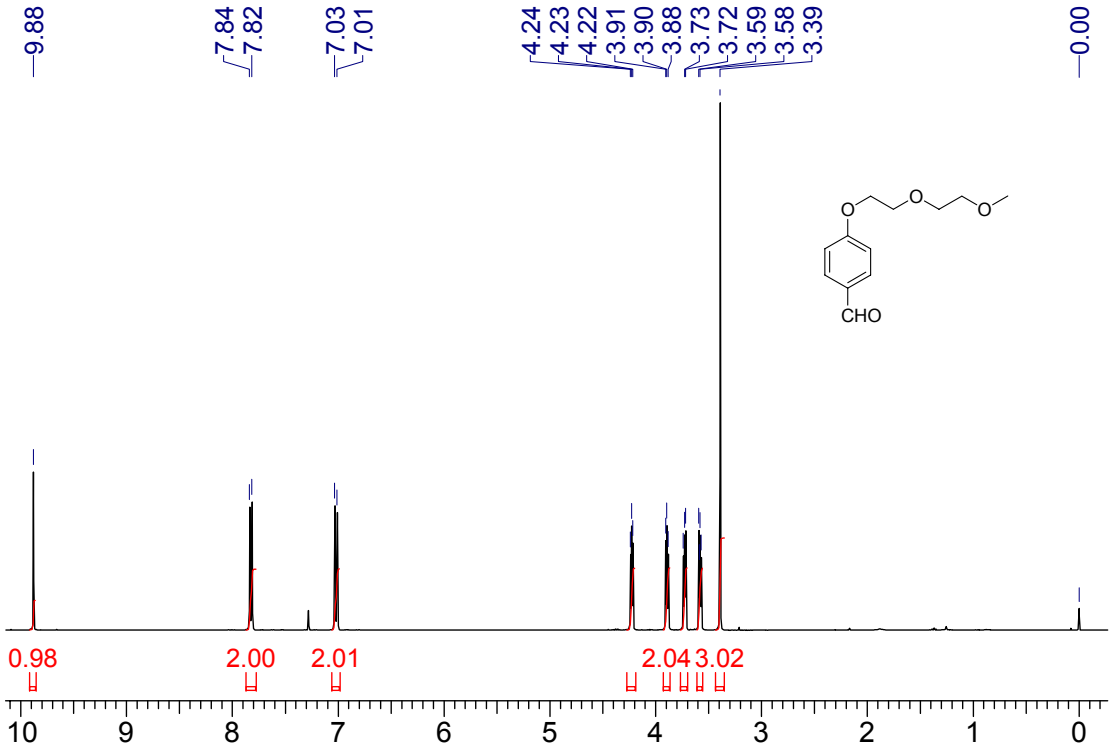

Figure S4. ^{1}H NMR of **2** ($CDCl_3$, 400 MHz).

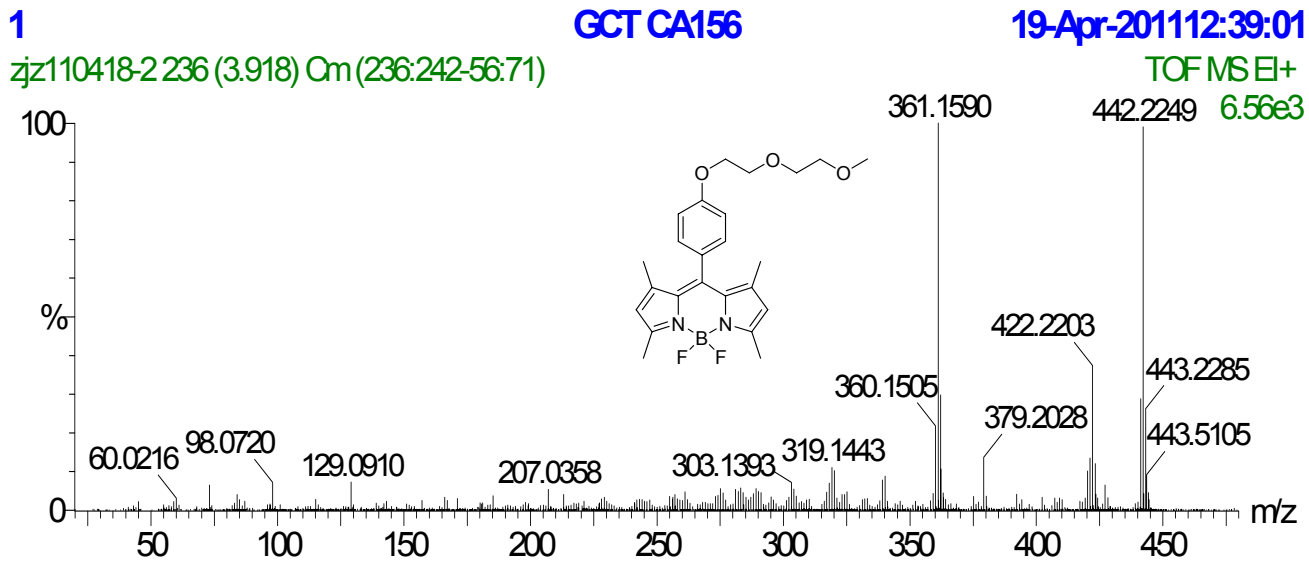

Figure S5. TOF MS EI of **3**.

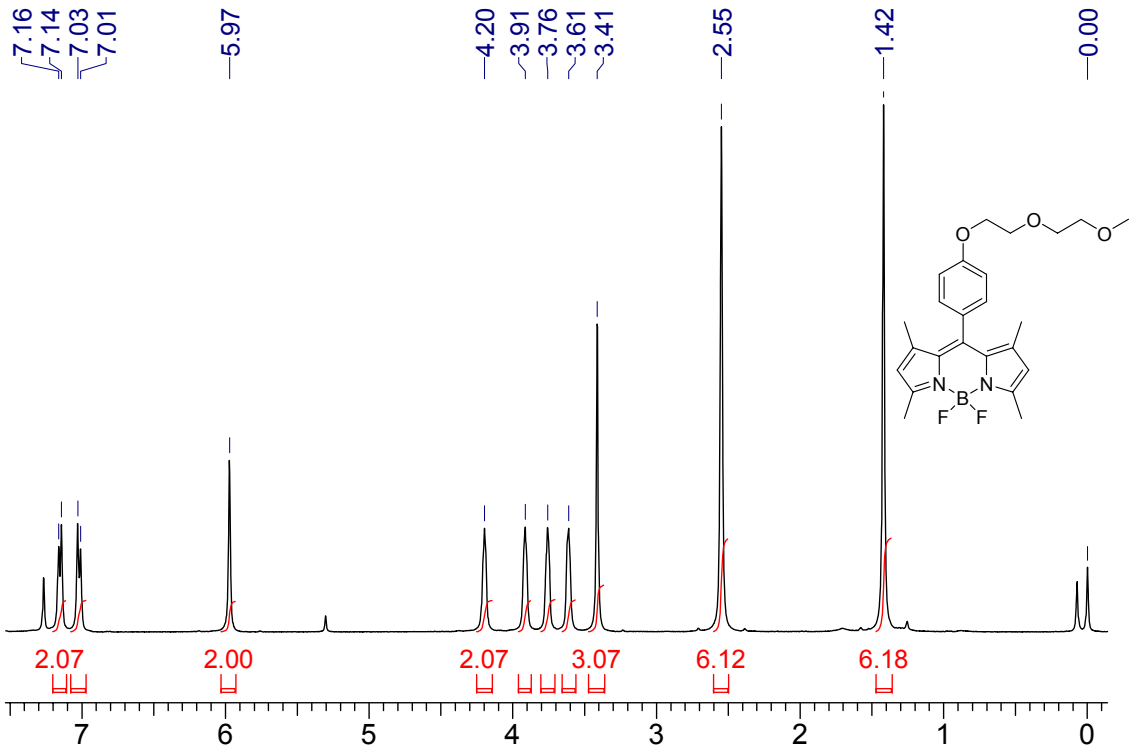

Figure S6. ^{1}H NMR of **3** ($CDCl_3$, 400 MHz).

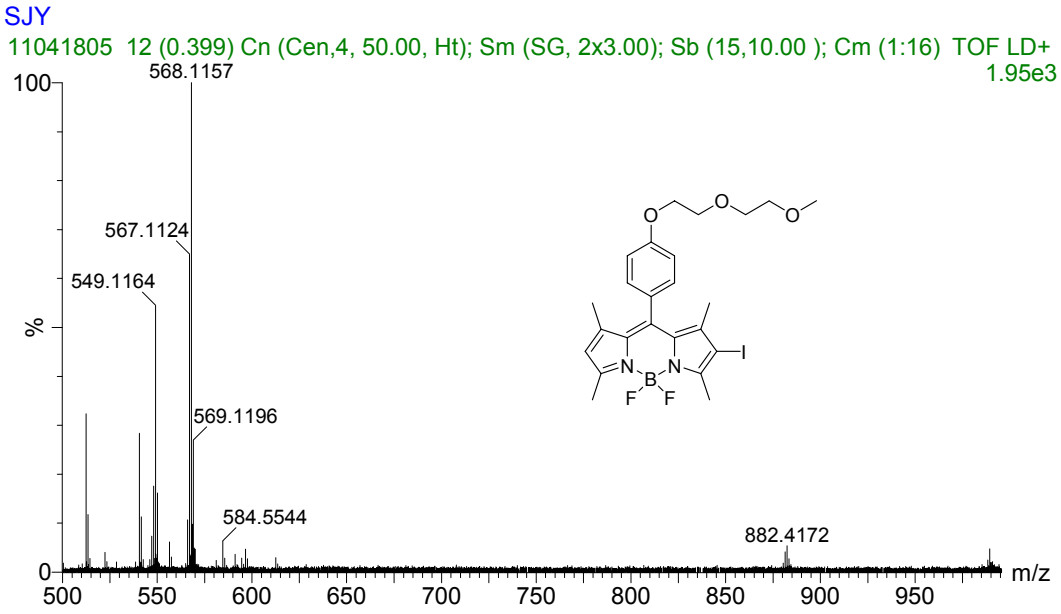

Figure S7. TOF MS EI of **4**.

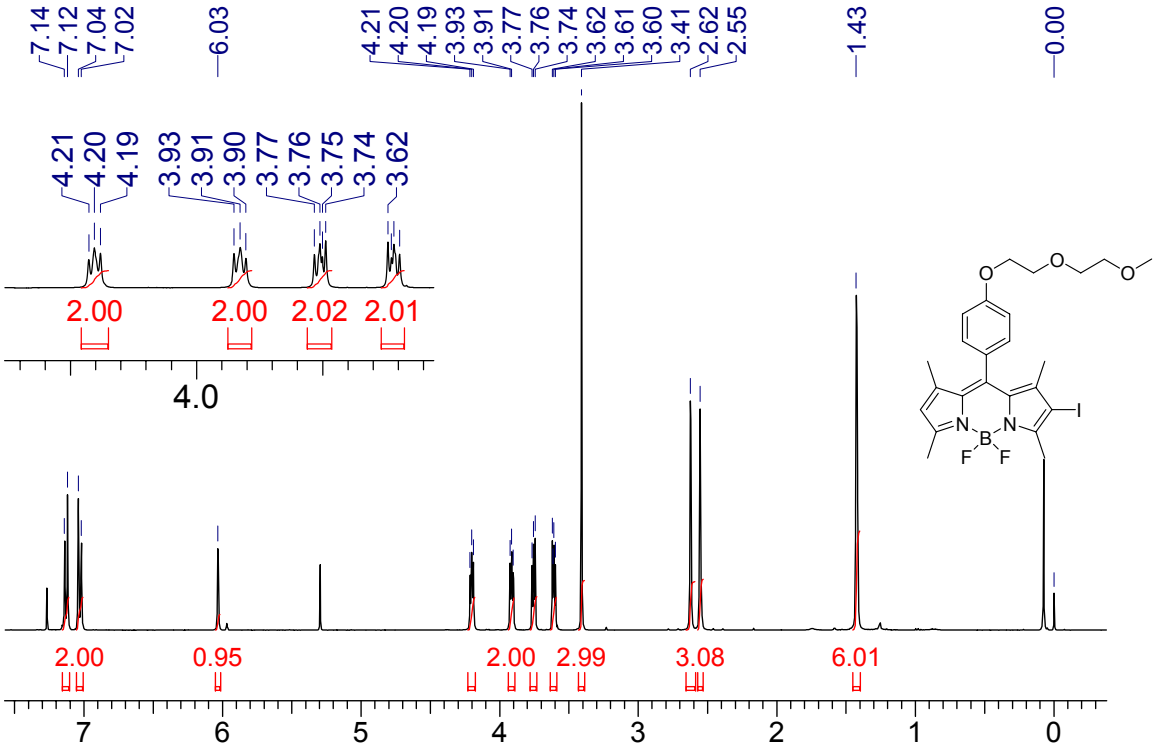

Figure S8. ^{1}H NMR of **4** ($CDCl_3$, 400 MHz).

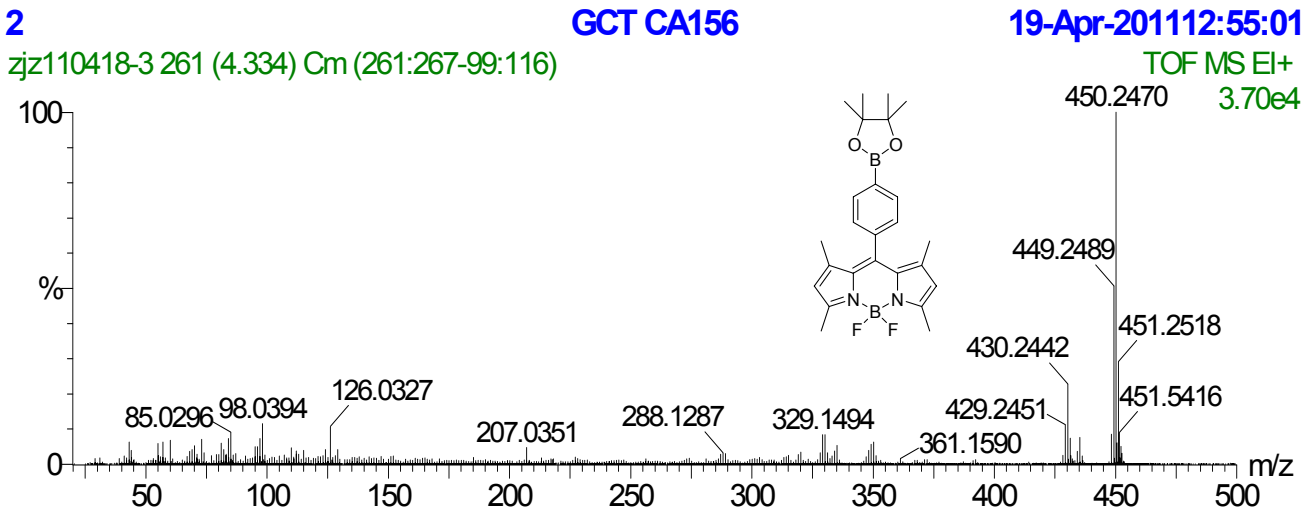

Figure S9. TOF MS EI of **5**.

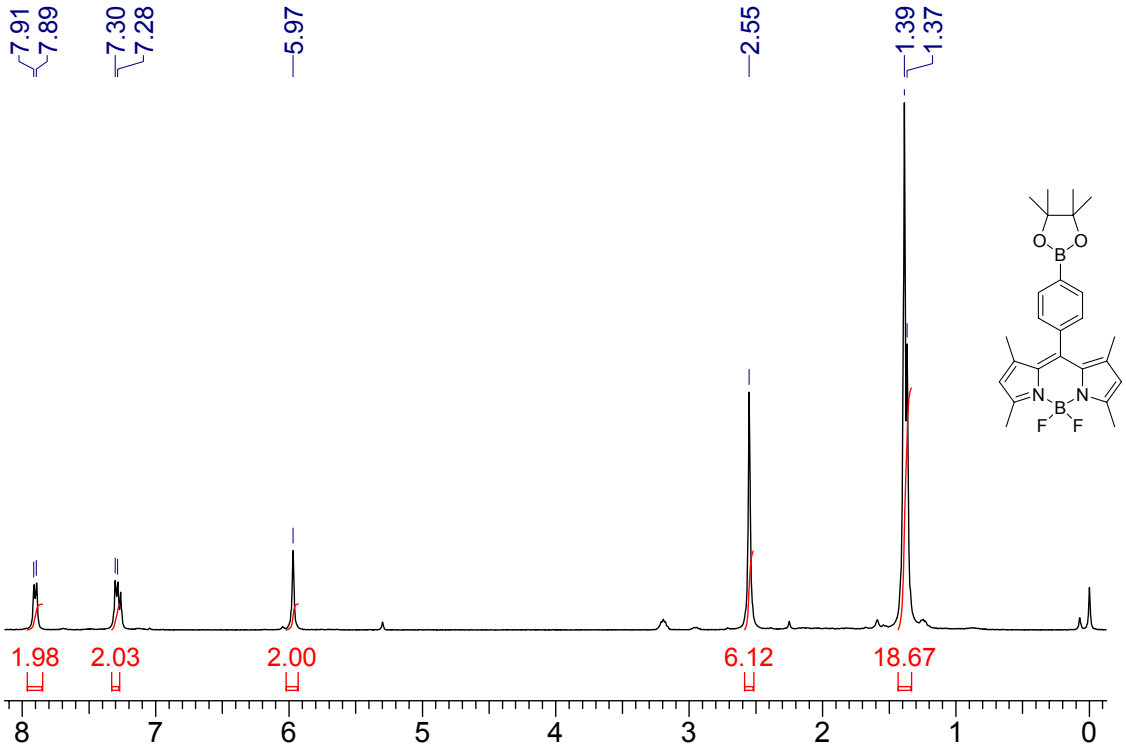

Figure S10. ^{1}H NMR of **5** ($CDCl_3$, 400 MHz).

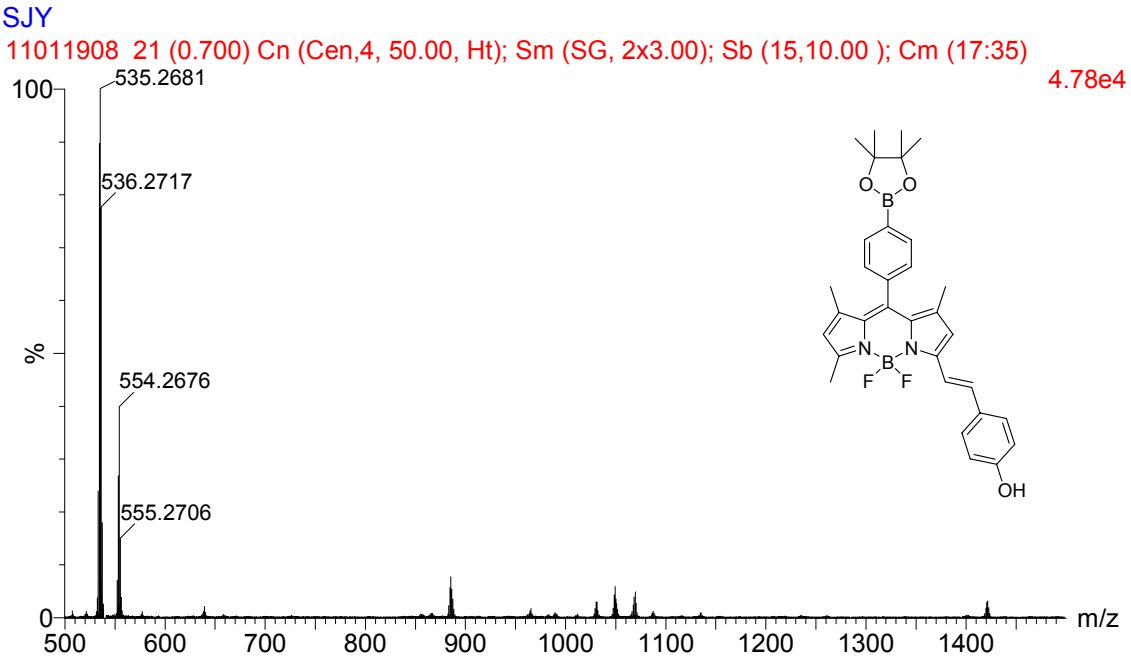

Figure S11. TOF LD of **6**.

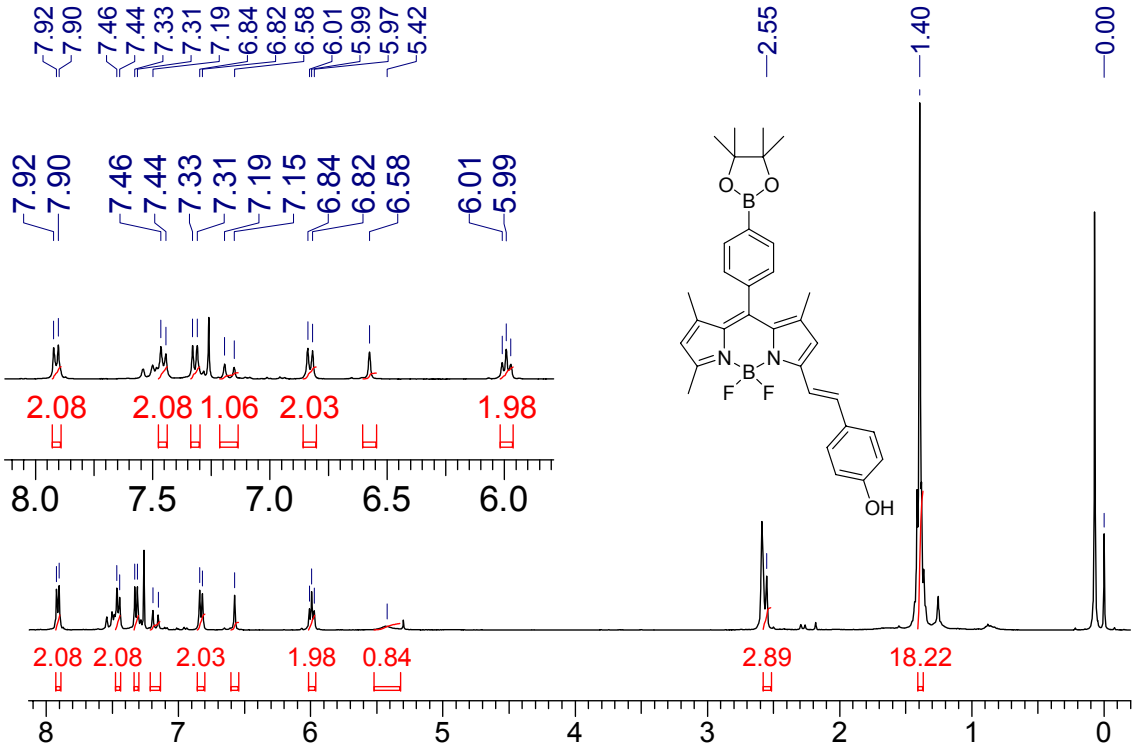

Figure S12. ^{1}H NMR of **6** ($CDCl_3$, 400 MHz).

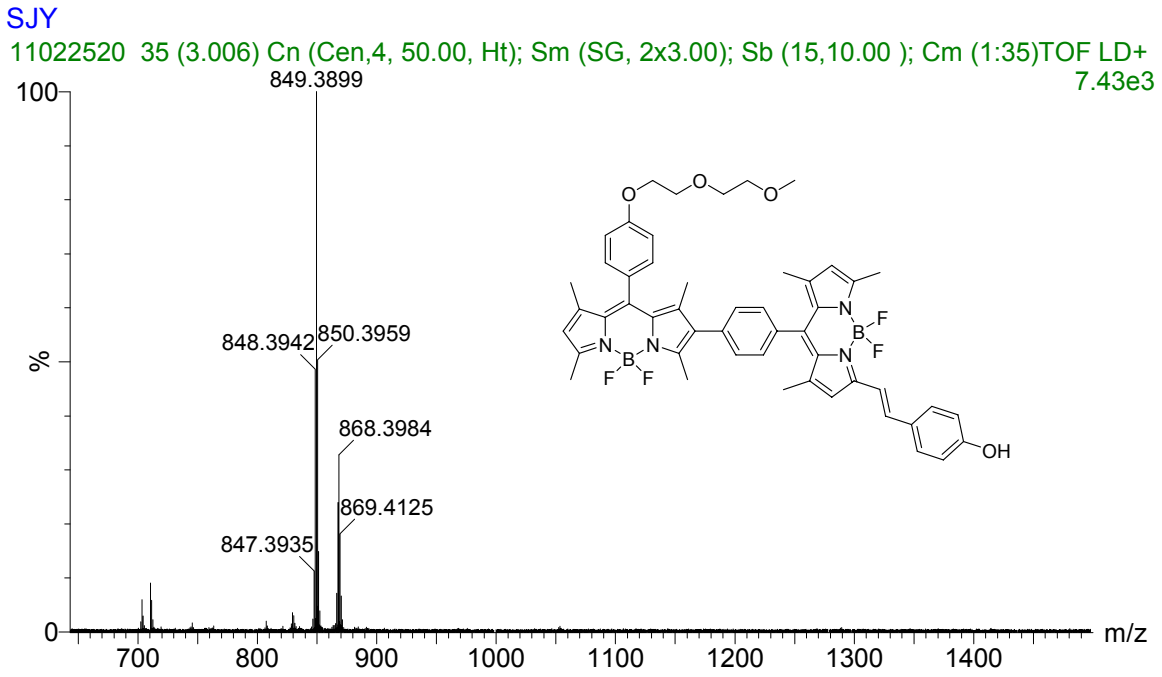

Figure S13. TOF LD of **7**.

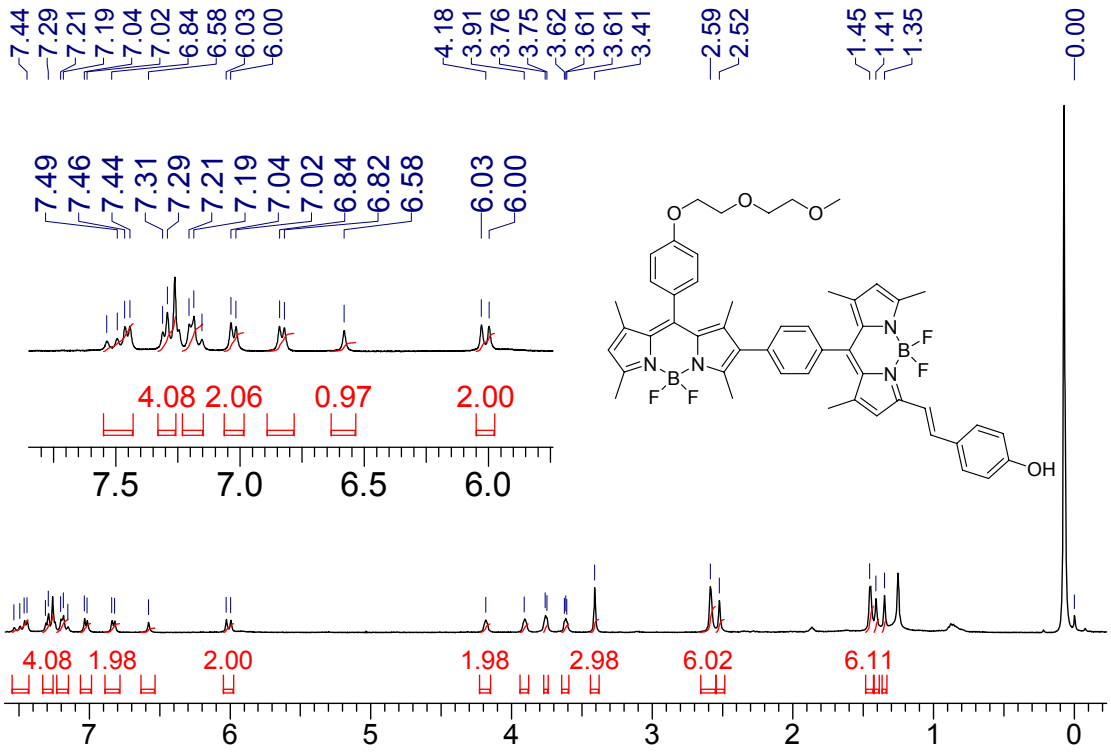

Figure S14. ^{1}H NMR of **7** ($CDCl_3$, 400 MHz).

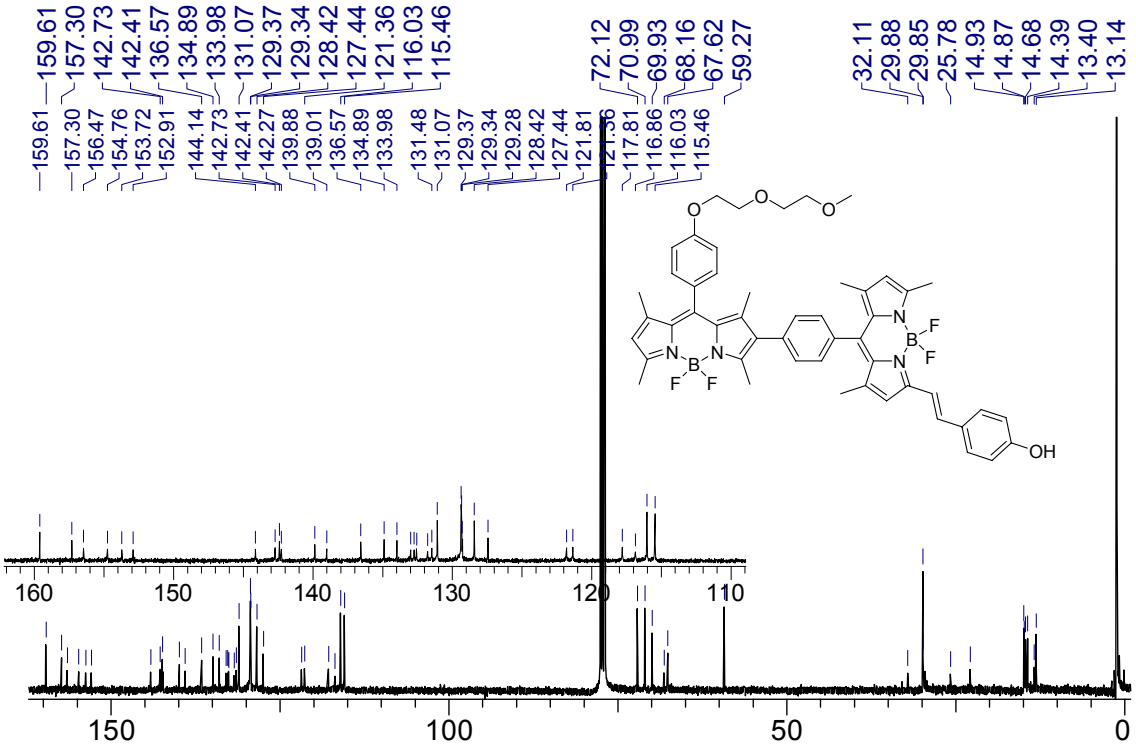

Figure S15. ^{13}C NMR of **7** ($CDCl_3$, 100 MHz).

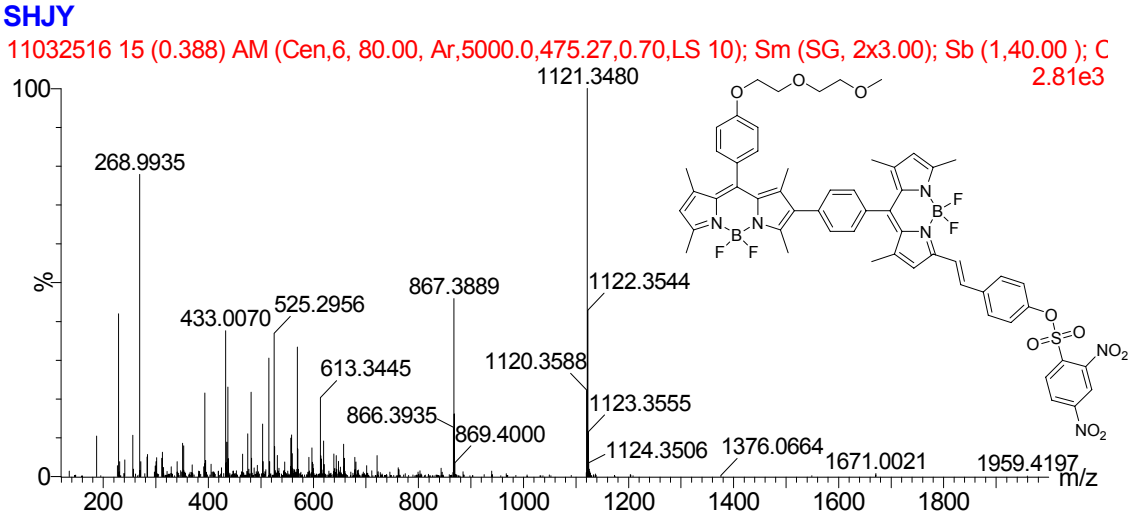

Figure S16. TOF MS EI of **Probe 1**.

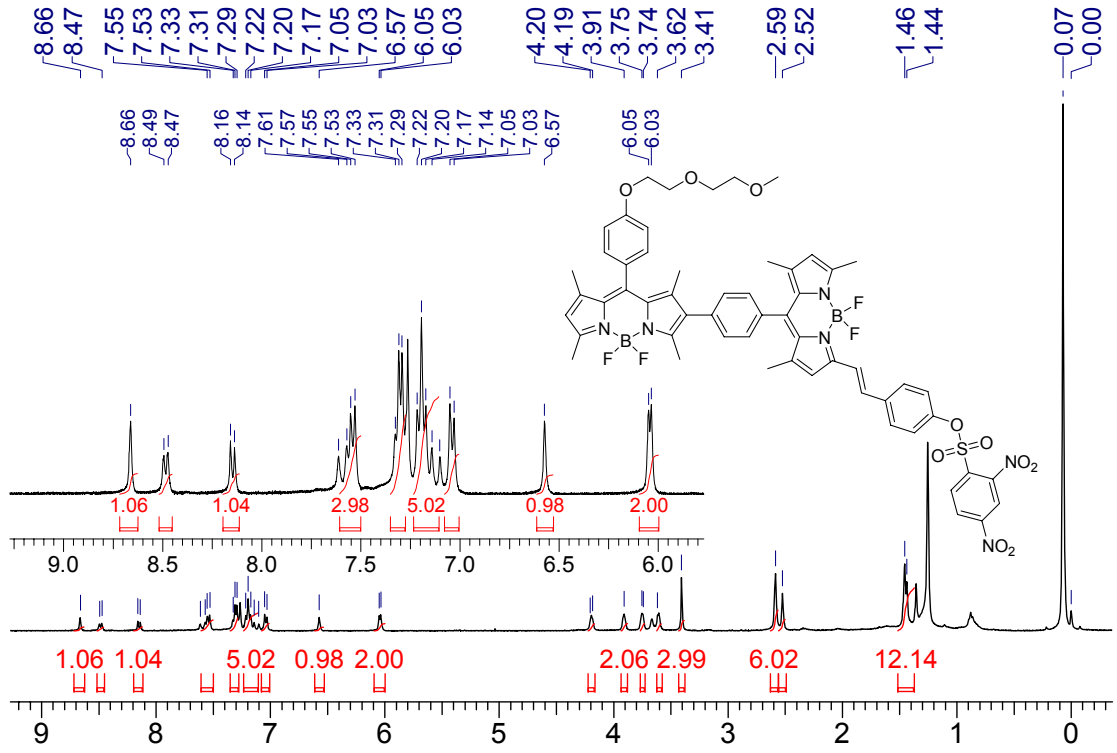

Figure S17. ^{1}H NMR of **Probe 1.** ($CDCl_3$, 400 MHz).

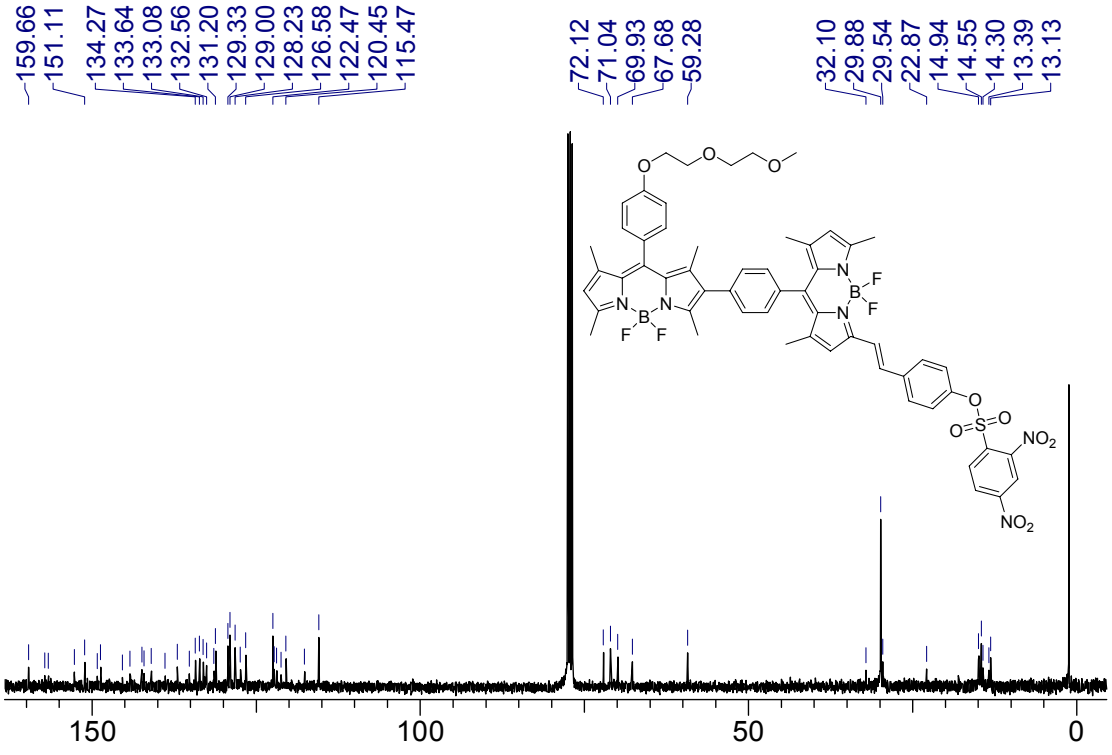

Figure S18. ^{13}C NMR of **Probe 1** ($CDCl_3$, 100 MHz).

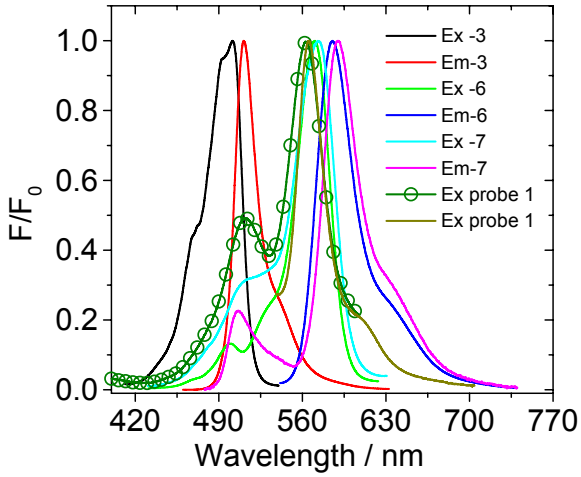

Figure S19. Relative fluorescence emission and excitation spectra of **3**, **6**, **7** and **Probe 1** in a mixture of MeOH/H_2O (V:V, 4:1). 25 ^{o}C.

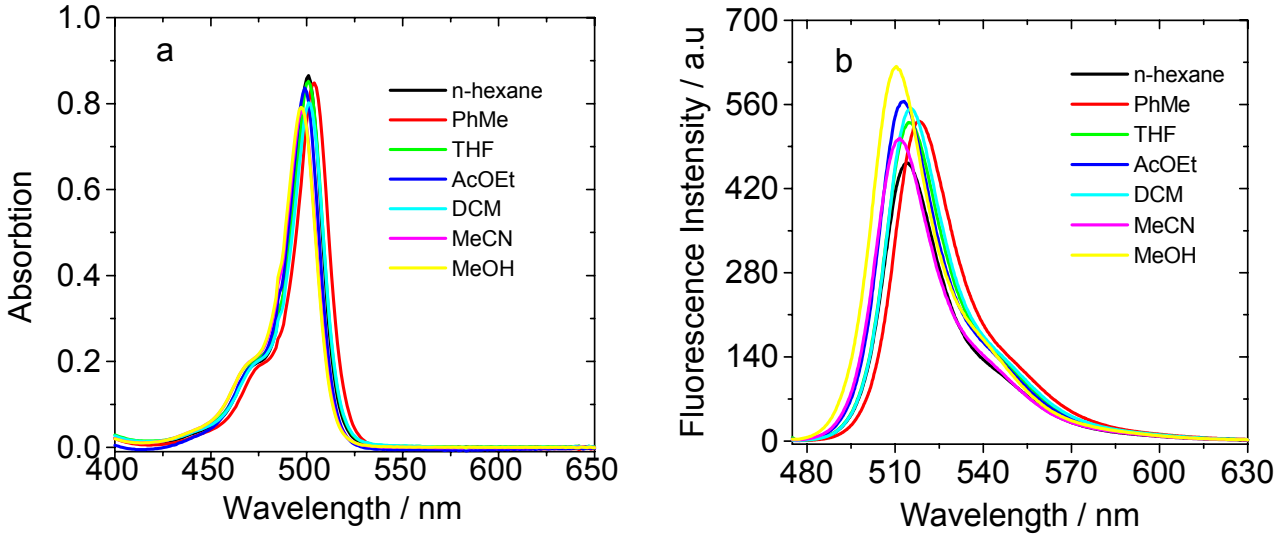

Figure S20. (a) The UV-Vis absorption of **5** in different solvents (c = 1.0 × 10^{-5} mol/L), 20 °C. (b) Fluorescence emission spectra of **5** in different solvents (c=1.0×10^{-5} mol/L, λ_{ex} = 470 nm), 20 °C.

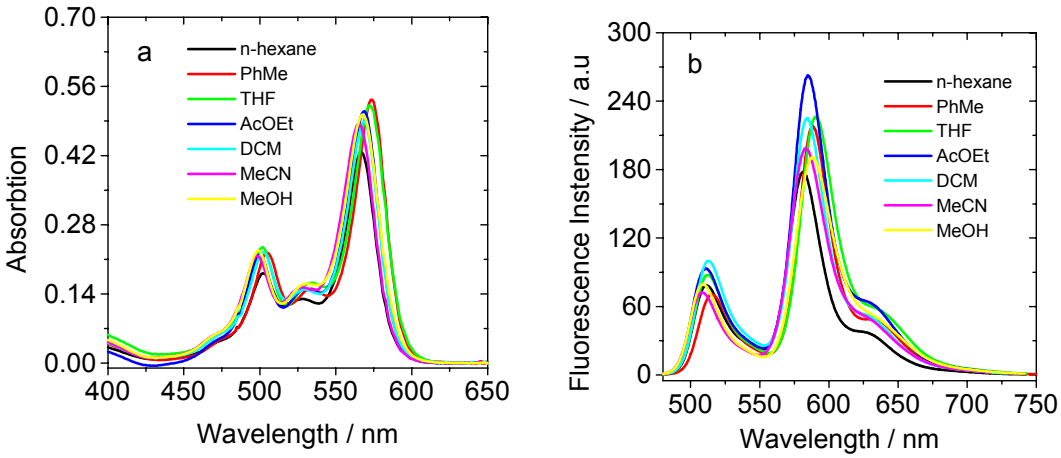

Figure S21. (a) The UV-Vis absorption of **6** in different solvents (c = 1.0 × 10^{-5} mol/L), 20 °C. (b) Fluorescence emission spectra of **6** in different solvents (c=1.0×10^{-5} mol/L, λ_{ex} = 470 nm), 20 °C.

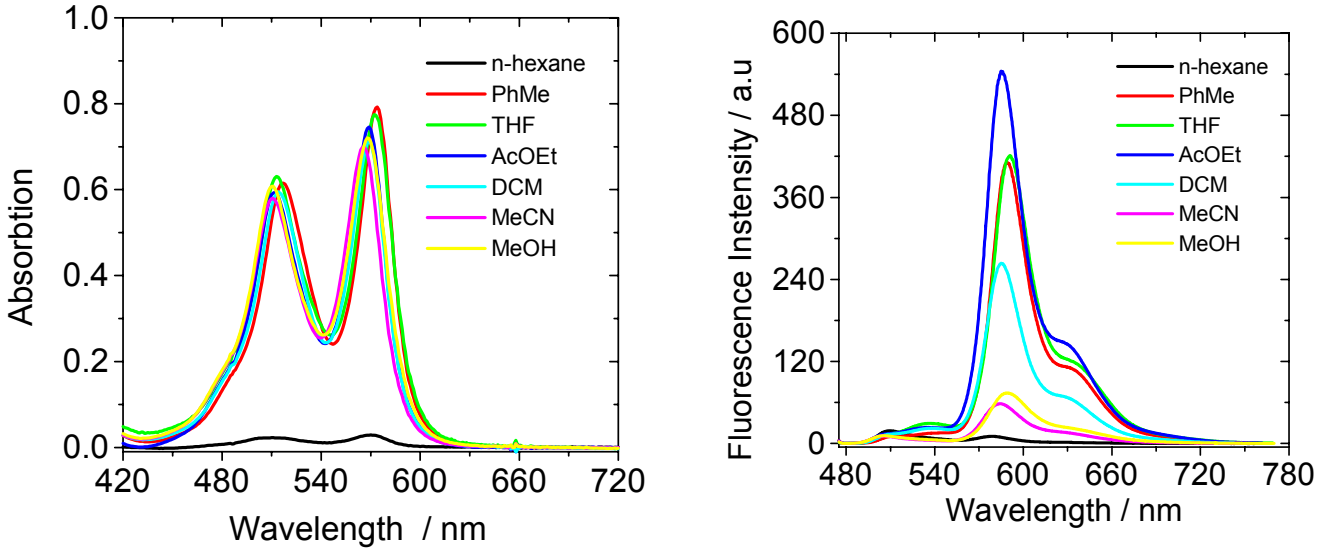

Figure S22. (a) The UV-Vis absorption of **7** in different solvents (c = 1.0 × 10^{-5} mol/L), 20 °C. (b) Fluorescence emission spectra of **7** in different solvents (c=1.0×10^{-5} mol/L, λ_{ex} = 470 nm), 20 °C.

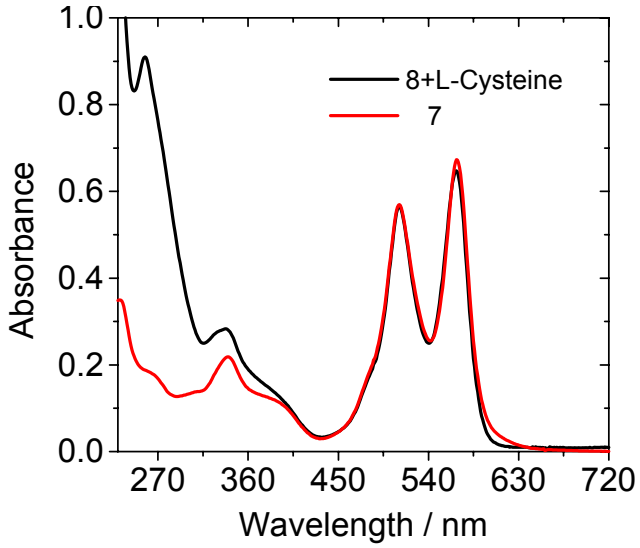

Figure S23. UV-Vis absorption of **7** and **Probe 1** after addition of L-cysteine. (MeOH/H_2O (4:1, v/v). c_{Probe} = 1.0 × 10^{-5} mol/L, $c_{(L\text{-cysteine})}$ = 3.0×10^{-3} mol/L. 37 °C)

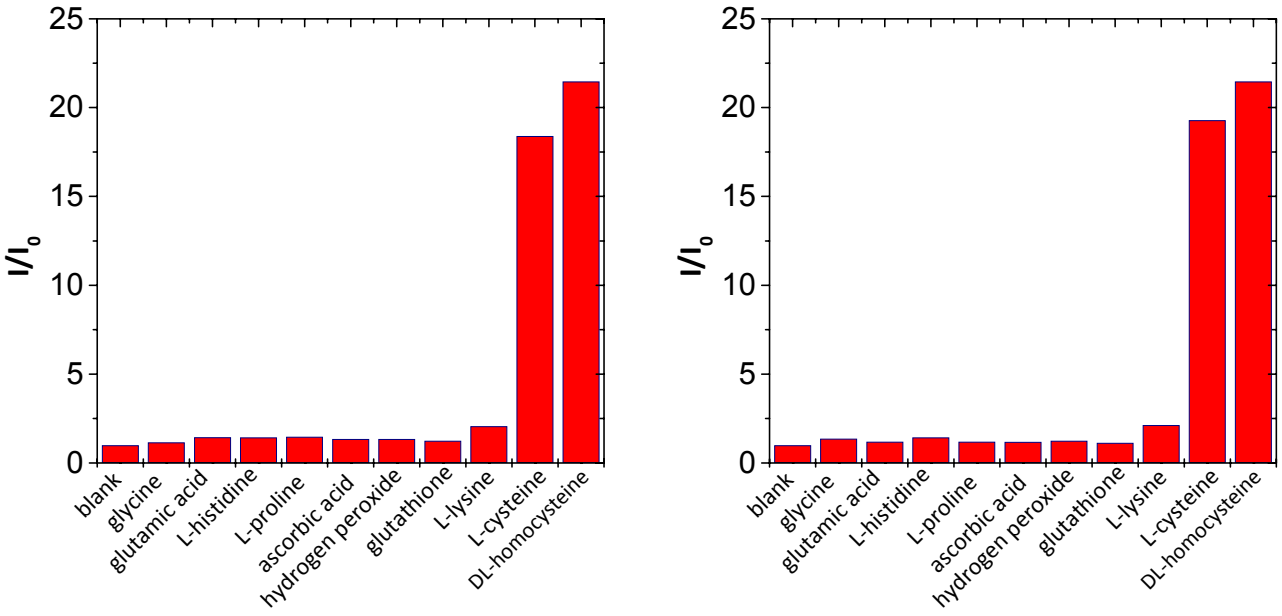

Figure S24. Response of **Probe 1** to different analytes. Relative fluorescence intensity of 10 μM probe at 590 nm (λ_{ex} = 505 nm) before and after incubation in the presence of 3.0×10^{-3} mol/L analyte at 37 °C. pH 7.4, MeOH : H_2O (V/V = 4⁄1).

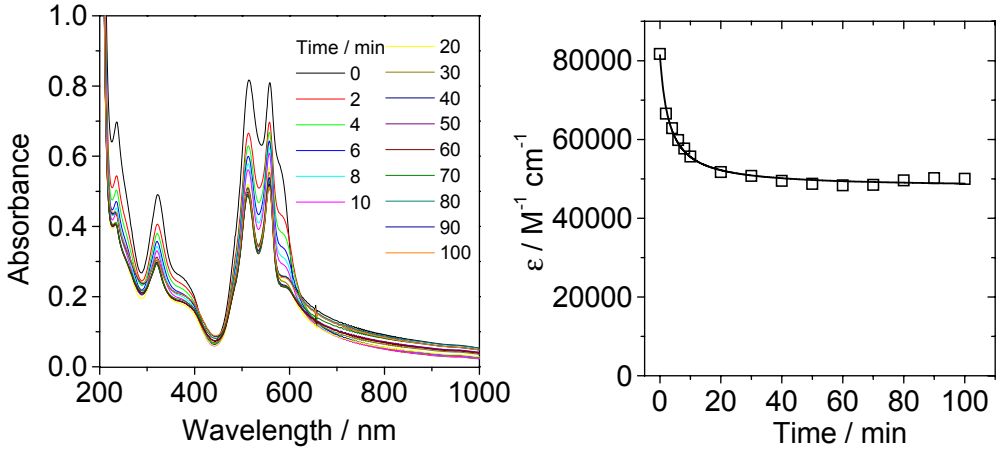

Figure S25. Photostability of the probe **1**, measured by (a) UV-vis spectral changes of probe 1 under illumination with 30 W Xenon lamp (Power density at the solution position: 57 w/m^2). (b) the evaluation of the molar extinction coefficients at 513 nm. In MeOH/H_2O (4:1, v:v). 25 °C.

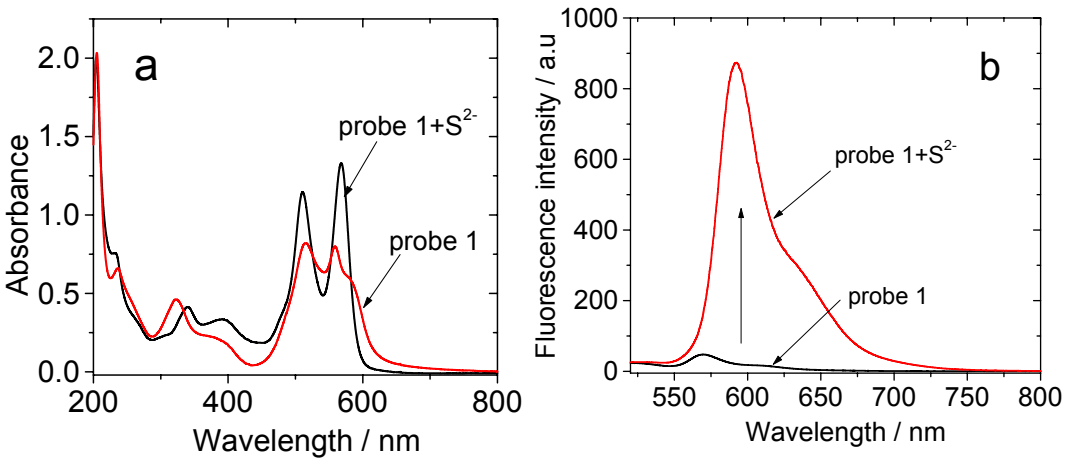

Figure S26. Response of probe **1** to Na_2S. (a) Uv-vis absorption spectra of probe **1** (10.0 μM) upon the addition of S^{2-} (10 equiv). (b) Emission spectra of probe 1 (10.0 μM) upon the addition of S^{2-} (10 equiv). The S2- was added as Na_2S. In MeOH/H_2O (4:1, v:v). 25 °C.

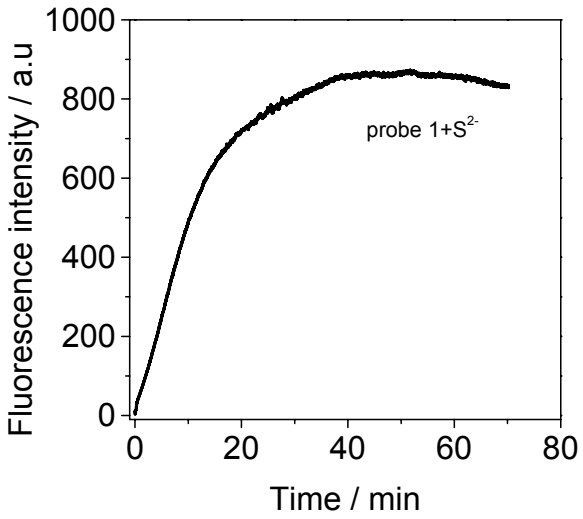

Figure S27. The sensing kinetics of probe **1** toward S^{2-}. In a mixture of MeOH/H_2O (4:1, v:v). $c_{[probe\ 1]} = 1.0 \times 10^{-5}$ mol/L, $c\ [S^{2-}] = 1.0 \times 10^{-4}$ mol/L. 25 °C.

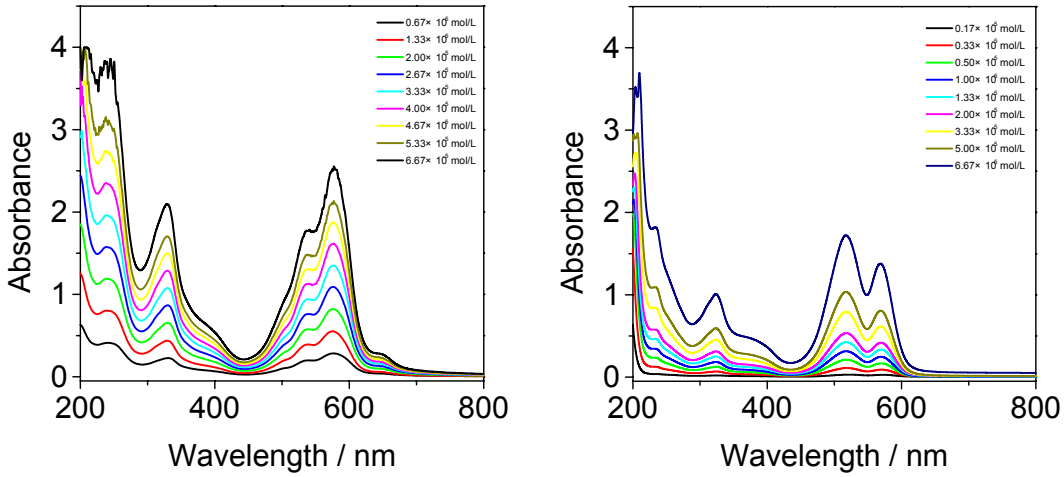

Figure S28. Solubility of the probes **1** and a control probe. The UV-vis spectral changes of the different concentration of probe **1** and the control probe in MeOH/H_2O (1:1, V:V). 25 °C.

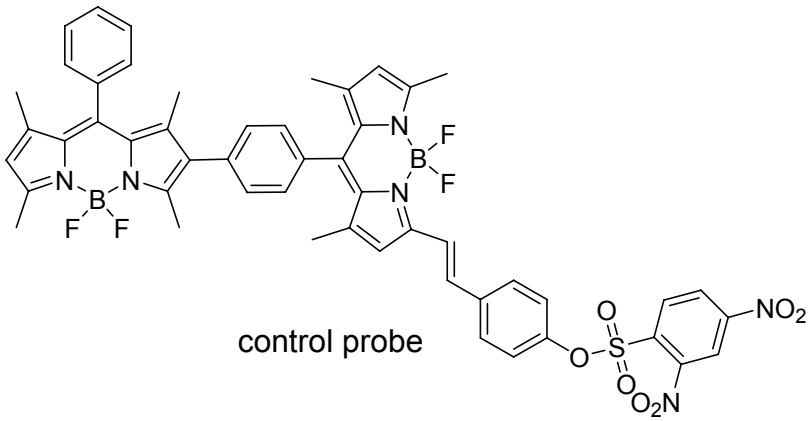

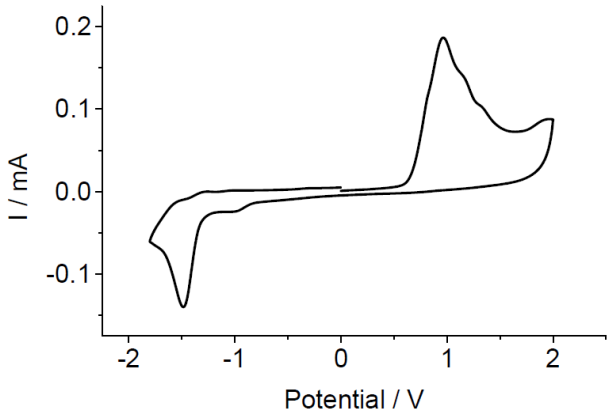

Figure S29. Cyclic voltammograms of probe **1** in CH_3CN at 20℃ using 0.1 M $^nBu_4BF_4$ as supporting electrolyte at a scan rate of 200 mV/S. Ferrocene is used as internal standard (half-wave potential = 0.06 V vs $Ag/AgNO_3$).

	E^{i0}_{ox},V (△E,mV)	E^{i0}_{red},V(△E,mV)	$E_{1/2}(F_c/F_c^+)$
1	0.97(irrev)	-1.50(irrev)	0.06